Published in final edited form as:
Brain Res. 2011 October 28; 1420: 1–7. doi:10.1016/j.brainres.2011.08.078.

Sleep loss alters synaptic and intrinsic neuronal properties in mouse prefrontal cortex

Bradley D. Winters, **Yanhua H. Huang**, **Yan Dong**, and **James M. Krueger**
Program in Neuroscience, Washington State University, Pullman, WA 99164-6520

Abstract

Despite sleep-loss-induced cognitive deficits, little is known about the cellular adaptations that occur with sleep loss. We used brain slices obtained from mice that were sleep deprived for 8 h to examine the electrophysiological effects of sleep deprivation (SD). We employed a modified pedestal (flowerpot) over water method for SD that eliminated rapid eye movement sleep and greatly reduced non-rapid eye movement sleep. In layer V/VI pyramidal cells of the medial prefrontal cortex, miniature excitatory post synaptic current amplitude was slightly reduced, miniature inhibitory post synaptic currents were unaffected, and intrinsic membrane excitability was increased after SD.

Keywords

sleep deprivation; prefrontal cortex; membrane excitability; EPSC; IPSC; synaptic; flowerpot

1. Introduction

The prefrontal cortex (PFC) mediates cognitive responses (Goldman-Rakic, 1995; Miller and Cohen, 2001; Robbins, 2005) that are sensitive to disruption by sleep loss. Following sleep deprivation (SD), memory, planning, decision-making, and other PFC-mediated cognitive abilities are impaired (Chuah, 2006; Thomas et al., 2000; Wu et al., 2006). Accompanying these post-SD behavioral alterations, the PFC exhibits larger increases in slow-wave (0.5-4.0 Hz) activity during sleep than other brain regions (Finelli et al., 2000; Mauzur et al., 2002), suggesting the PFC is disproportionately affected by SD (Steriade, 2006). Indeed, the generation of high amplitude electroencephalogram (EEG) slow-waves is initiated in the PFC and then extends to other cortical areas (Massimini, 2004).

A great deal is known about impairment of PFC function by sleep loss in humans (Killgore, 2010); however less is known about how these processes are affected in rodents as higher cognition is more difficult to measure in these animals. Nonetheless, memory is clearly impaired by sleep loss in tasks that are hippocampus dependent, but also critically involve

Corresponding Author: James M. Krueger: Program in Neuroscience, Washington State University Address: WWAMI Medical Education Program Health Sciences Building, Room 280M PO Box 1495 Spokane, WA 99210-1495 krueger@vetmed.wsu.edu Phone: 509-358-7808 Fax: 509-358-7627 .
bwinters@vetmed.wsu.edu
yhuang@vetmed.wsu.edu
yandong@vetmed.wsu.edu

the medial PFC (mPFC) for consolidation (Marshall and Born, 2007; Nieuwenhuis and Takashima, 2011). In rats, 4 h of flowerpot SD is sufficient to impair performance in the Morris water maze (Le Marec et al., 2001; Smith and Rose, 1996). In mice, 6 h of SD by the gentle handling method impairs object recognition memory (Palchykova et al., 2006). Also in mice, 5 h of gentle handling SD impairs consolidation of fear conditioning (Graves, 2003).

Despite evident effects on PFC function, it remains poorly understood how sleep loss affects basic properties of PFC neurons. To begin to address this knowledge gap, we examined the impact of SD on synaptic input and membrane excitability. The integration of these two parameters determines the overall functional output of PFC neurons (Hille, 2001).

We focused on pyramidal neurons located in layers V and VI of the mPFC. These neurons are particularly important for planning, attention, working memory, and other cognitive responses, because they coordinate and direct output to other cortical regions as well as the dorsal and ventral striatum (Berendse et al., 1992; Groenewegen et al., 1990; Groenewegen and Uylings, 2000; Sesack et al., 1989).

We show herein that following SD, miniature excitatory postsynaptic currents (mEPSCs) and miniature inhibitory postsynaptic currents (mIPSCs) were either slightly altered or unchanged. Along with these synaptic effects, SD increased the intrinsic membrane excitability of mPFC neurons. Taken together, these SD-induced synaptic and membrane alterations suggest that following SD, mPFC neurons may exhibit higher activity levels. The relevancy of increased PFC pyramidal cell membrane excitability to function remains to be determined; it may represent a compensatory mechanism by which the brain attempts to maintain a functional output or, conversely, it may be a cellular manifestation of the dysfunctions associated with sleep loss.

2. Results

2.1. Use of the pedestal method for acute sleep deprivation

To determine the effectiveness of the pedestal method for short-term SD, we made EEG recordings of mice subjected to pedestal SD for 8 h (n=8). Baseline recordings for 24 h were made, then 24 h recordings were made from the same animals beginning at the start of the SD period (Fig. 1). As expected, pedestal SD eliminated rapid eye movement (REM) sleep (2-factor ANOVA with repeated measures, significant main effect of treatment $F_{1,7}$=14.55, p=0.007, Fig. 2B). The animals exhibited only 46% of baseline non-rapid eye movement (NREM) sleep during the SD period (Fig. 2A) and displayed a moderate rebound in both REM and NREM sleep (2-factor ANOVA with repeated measures, significant main effect of treatment $F_{1,7}$=23.32, p=0.002, Fig. 2A) during the first 5 h after SD (Fig. 2A,B). We did not observe REM sleep rebound in excess of loss as occurs after some stressors (Bodosi et al., 2000). After SD, the mice exhibited a substantial rebound over baseline in NREM sleep delta power (2-factor ANOVA with repeated measures, significant interaction effect of treatment*time $F_{23,161}$=3.45, p<0.001, Fig. 2C). This effect was limited to the first 3 h after SD. Analysis of the NREM power spectra for the first 1 h after SD revealed that the increase in power was mainly in the 0.5 to 3 Hz range (2-factor ANOVA with repeated measures, significant interaction effect of treatment*time $F_{39,273}$=2.28, p=0.001, Fig. 2D).

Since mice used for patch clamp recordings would not be equipped with EEG tethers, a group of animals were disconnected from their tethers during SD and reconnected to record their recovery period. These animals (n=4, data not shown) exhibited similar rebounds in sleep time and EEG delta power as animals that remained tethered. Video recordings during pedestal SD were made of untethered animals (n=6, data not shown). Using these recordings

we observed that the animals remained quite active for 8 h, often switching between pedestals, and frequently fed on the provided food pellet.

2.2. Synaptic effects of SD

The effects of SD on excitatory synaptic efficacy were measured by examining mEPSCs (control: n=15 cells, 5 animals; SD: n=15 cells, 4 animals). Although the average mEPSC amplitude was lower in the SD group, it was not significantly different (p=0.16, control vs. SD, t-test, Fig. 3A, C). However, the cumulative frequency distribution of these mEPSC amplitudes after SD was significantly shifted toward lower amplitudes ($p<0.001$, Kolmogorav-Smirnov test, Fig. 3D). The average mEPSC frequency was not affected by SD ($p>0.05$, t-test, Fig. 3A, B).

The effects of SD on inhibitory synapses were assessed by measuring mIPSCs in another set of animals (control: n=24 cells, 4 animals; SD: n=20 cells, 4 animals). Neither the average frequency nor average amplitude were different ($p>0.05$, control vs. SD, t-test, Fig. 3E, F, G). The cumulative frequency distributions of these mIPSCs were also not significantly different between the SD and control groups (p=0.25, Kolmogorav-Smirnov test, Fig. 3H)

2.3. Membrane effects of SD

The intrinsic membrane excitability of mPFC neurons was assessed by measuring and comparing the evoked action potential (AP) firing in control and SD-treated mice (control: n=22 cells, 7 animals; SD: n=27 cells, 6 animals). The evoked AP firing (injected current steps from 75 to 225 pA from a membrane potential near −70 mV) was significantly higher in the SD-treated mice than in control mice (two-factor ANOVA, main effect of treatment $F_{(1,329)}=8.16$, p=0.005, Fig. 4A, B), suggesting that SD increases the intrinsic excitability of deep layer mPFC neurons. To attempt to gain insights into the ionic basis underlying SD-induced upregulation of membrane excitability, we compared averaged AP afterhyperpolarizations (AHPs) between control and SD groups (data not shown) and found no differences. We performed an analysis of the sag ratio in response to hyperpolarizing currents (data not shown) and found there was no effect of SD. We also measured and compared the general membrane properties of mPFC neurons between control and SD-treated mice. No significant alterations were detected in any membrane parameters that we examined (Table 1), but the modest decrease in AP threshold (p=0.13, t-test) and increase in input resistance (p=0.27 at −100 pA, t-test) we observed would contribute increased excitability. The lack of significant regulation of any single parameter measured suggests that the observed effects of SD on membrane excitability may not be mediated by a single type, but by a combination of moderately modulated ionic conductances.

3. Discussion

The flowerpot or pedestal over water method of SD has traditionally been used with rodents for long periods of REM sleep deprivation (Davis et al., 2006; McDermott et al., 2003). The method is effective because the animal will fall from the pedestal due to muscle atonia upon entering REM sleep, and thus be awakened. The pedestal method was indeed very effective at eliminating REM sleep. Additionally, we found that this method substantially reduced NREM sleep as well during relatively short (8 h) sessions in mice (Fig. 2A). Short-term pedestal SD should be considered a rather mild method of SD because it allows the animals to obtain some NREM sleep; nonetheless, a clear NREM sleep and delta power as well as REM sleep rebound were evident (Fig. 2), suggesting that sleep need or homeostatic drive for sleep was substantially generated. The pedestal method has the advantage of requiring less involvement of the experimenter; thus, is more objective and potentially less stressful, although we did not directly investigate stress levels.

After SD, there was a modest but significant decrease in the amplitude of mEPSCs impinging on deep-layer mPFC neurons (Fig. 3D), suggesting a post-synaptic decrease in α-amino-3-hydroxy-5-methyl-4-isoxazolepropionic acid (AMPA) receptors (Turrigiano et al., 1998). This contrasts with a recent report in which an increase in both the amplitude and frequency of mEPSCs was observed in neurons within layer II/III of the frontal association cortex from rats and mice after 4 h SD by gentle handling (Liu et al., 2010). The SD protocol used in this case was especially mild since these animals were not disturbed for the first 2 h after light onset when NREM sleep is most intense. These seemingly discrepant results may reflect that SD differentially regulates discrete brain regions rather than simply exerting across-the-board effects on the brain (Crick and Mitchison, 1983; Krueger and Obal, 1993; Tononi and Cirelli, 2006). To extend this notion, the layers of the cerebral cortex are thought to represent discrete functional networks (Grossberg, 2006). In the PFC, layers V and VI are thought to integrate and organize output, whereas layers II and III are thought to mainly be involved in processing (Berendse et al., 1992; Groenewegen et al., 1990; Groenewegen and Uylings, 2000; Sesack et al., 1989). Thus, the differential effects of SD on different cortical regions and layers may contribute to distinct aspects of SD-induced behavioral alterations.

Recently it was reported that burst firing patterns, reminiscent of those occurring during NREM sleep, induced by current injections into somatosensory layer V pyramidal cells resulted in depression of AMPA receptor-mediated currents (Lante et al., 2011). By inference, reducing NREM sleep would inhibit normal removal of AMPA receptors leading to their accumulation. If that is the case, although not experimentally demonstrated, the Lante *et al*. results would be inconsistent with our current result that sleep restriction depressed mEPSC amplitudes. Further, Lante *et al.* did not examine whether overall AMPA-mediated currents were larger with higher sleep pressure at the end of the dark period.

Evoked AP firing rates were higher following SD, suggesting an adaptation toward higher intrinsic membrane excitability (Fig. 4). This result is consistent with a recent report showing a similar increase in excitability of deep-layer PFC pyramidal cells from rats following 4 h of gentle handling SD (Yan et al., 2011). Our work is further consistent with Yan (2011) in that the fast AHP and sag ratio in response to hyperpolarizing current were not affected by SD. However, our analysis of the later AHP did not reveal the decrease in AHP associated with SD found by Yan and colleagues. Possible reasons for this discrepancy include species differences and the SD protocol used. Perhaps the amount of NREM sleep acquired by the animals in the present study is sufficient to mask or reduce AHP differences below detection levels. Results seemingly similar to our finding of increased excitability with SD were observed in layers II, III and V (pooled together) of the barrel cortex of intact rats, in which the average unit spontaneous AP firing frequency is increased following SD (Vyazovskiy et al., 2009). However, this observed effect in the barrel cortex could also be mediated by SD-induced synaptic alteration such as an increase in excitatory synaptic input as has been suggested for other cortical regions (Liu et al., 2010).

Our observed effect of SD on PFC neurons in layer V/VI is opposite to that observed in subcortical neurons, such as rat hippocampal CA1 neurons, in which SD induces substantial downregulation of intrinsic membrane excitability (McDermott, 2005; McDermott et al., 2003; Yang et al., 2010). These authors used a multiple platform method of SD similar to the method used here; however, the SD period was for 72 h. Tartar and colleagues also reported a decrease in rat hippocampal excitability with 24 h of sleep fragmentation (Tartar et al., 2010). Despite differences in SD duration and methodology, these observations in contrast with our observation of increased cortical excitability demonstrate that different brain sites respond to sleep loss in different ways. This inference is consistent with the

interpretation that local site-specific activity-dependent sleep loss-associated cellular changes occur (Krueger et al., 2008).

Our findings at the synaptic and membrane levels would have opposite effects on integrated output. This implies that in this system the effects of SD may strive to counteract each other functionally to some degree. Nonetheless, a shift of synapse-membrane interaction toward higher excitability may adjust the gain of the input/output of PFC neurons as they perform cognitive tasks. For example, during evaluating or selecting tasks, previously sub-threshold and thus "silent" excitatory inputs that otherwise cannot activate PFC neurons may become capable of exciting PFC neurons, thus decreasing the signal-to-noise ratio. Clearly, a detailed understanding of the cellular basis of sleep-mediated regulation of PFC-based cognitive responses demands more extensive, in particular, *in vivo* studies. The SD-induced effects on basic neuronal properties characterized here in the PFC do provide initial cellular groundwork for more sophisticated *ex vivo* and *in vivo* manipulations in future studies.

4. Methods and Materials

4.1. Experimental animals

Male C57BL/6 mice 5 to 11 weeks old were used in this study (Simonsen Labs). Mice were maintained at room temperature (22 ±2°C), on a 12:12-h light-dark cycle (lights on 00:00, lights off 12:00), and individually housed with constant access to food and water. All animal procedures were approved by the Washington State University Institutional Animal Care and Use Committee.

4.2. Sleep recordings

For surgeries, mice were anesthetized with intraperitoneal ketamine and xylazine (87 and 13 mg/kg, respectively). A stainless-steel wire elecromyogram (EMG) electrode was inserted into the nuchal neck muscle and three gold-plated wire EEG electrodes (Plastics One, Roanoke, VA) were installed through the skull over the parietal and frontal cortices, as previously described (Krueger et al., 1993; Szentirmai et al., 2009). Electrode leads were gathered into a plastic socket (Plastics One) and fixed to the skull with dental cement (Patterson Dental Supply, Saint Paul, MN). Animals were connected to the amplifiers via lightweight cables and commutators (Plastics One). For habituation, the cables were connected to the mice for one week prior to experimental recordings.

Signals were amplified using Grass model 7P511 amplifiers (Grass-Telefactor, West Warwick, RI). The EEG was filtered below 0.1 Hz and above 100 Hz. The EMG was filtered below 30 Hz and above 3 kHz. All signals were digitized at 128 Hz and collected using Sleep Analysis software (Biosoft Studios, Hershey, PA) and visually scored for sleep state in 10 s epochs using Sleep Sign for Animal software (Kissei Comtec, Nagano, Japan) as previously described (Kapas et al., 2008; Krueger et al., 1993). Briefly, REM sleep is typically identified by a loss of muscle tone and a very regular low amplitude EEG with a large theta (6-9 Hz) frequency component. NREM sleep EEG typically has high amplitude and regular delta (0.5-5 Hz) frequency oscillations. Wakefulness produces a more irregular and generally low amplitude EEG, often accompanied by muscle activity (Fig. 1C).

4.3. Sleep deprivation

A modified pedestal or flowerpot method was used for SD. Mice were deprived of sleep for the 8 h following light onset (00:00-08:00, Fig. 1B). During the SD procedure, animals were placed on pedestals in a 50 cm deep plastic tub containing water 1.5 cm deep. The water was kept warm (30°C) using electric heating pads placed under the tub. The three plastic pedestals protruding from the bottom of the tub were 2 cm diameter, 6.5 cm high, and

separated by 7.5 cm (Fig. 1A). Having 3 pedestals that the animal could easily move between served to limit immobility. A standard food pellet was suspended from a thread near one of the pedestals. Animals were habituated to the pedestals and the environment for 2 h at least one day prior to the experimental day.

4.4. Patch clamp recordings

Mice for these experiments were sacrificed immediately following the SD period. Control mice remained in their home cages without disturbance and were killed at the same time of day as SD animals. Control mice were killed within 5 minutes of arousal. Animals were deeply anesthetized with isoflurane, decapitated, and the brain quickly removed. Coronal slices including the mPFC (Paxinos and Franklin, 2001) (Fig. 1D) were prepared as previously described (Huang et al., 2009; Ishikawa et al., 2009). Briefly, slices were cut on a Leica V1200 vibrating microtome 250-300 μm thick in an ice-cold oxygenated cutting solution (in mM: 135 NMDG, 1 KCl, 1.2 KH_2PO_4, 1.5 $MgCl_2$, 0.5 $CaCl_2$, 20 choline bicarbonate, 10 glucose, 295–305 mOsm, equilibrated with 95% O_2/5% CO_2), then submerged in 36°C oxygenated standard artificial cerebral spinal fluid (ACSF, in mM:126 NaCl, 1.6 KCl, 1.2 NaH_2PO_4, 1.2 $MgCl_2$, 2.5 $CaCl_2$, 18 $NaHCO_3$, 11 glucose, 285–295 mOsm, equilibrated with 95% O_2/5% CO_2) for 30 minutes, then stored at room temperature with constant oxygenation until being transferred to the recording chamber. During recordings, slices were constantly perfused with oxygenated ACSF at 30°C via an inline solution heater (Harvard Apparatus, Holliston, MA). Recordings were selectively made in layer V/VI of the infralimbic region of the mPFC (Fig. 1D). Pyramidal cells were preferentially targeted based on soma shape, large size, and dendritic polarity, if visible, using differential interference contrast microscopy (Olympus, Center Valley, PA). Whole-cell patch-clamp recordings were made using a Multiclamp 700B amplifier and Digidata 1440A digitizer (Molecular Devices, Sunnyvale, CA) through borosilicate glass electrodes (3-5 MΩ) and recorded at 20 kHz using Clampex 10.2 software (Molecular Devices, Sunnyvale, CA). Only stable cells with access resistances <25MΩ were included in data analyses.

Voltage-clamp recordings were used to measure mEPSCs and mIPSCs in separate sets of animals. For these recordings, pipettes were filled with cesium-based solution (in mM: 117 cesium methanesulfonic acid, 20 HEPES, 0.4 EGTA, 2.8 NaCl, 5 TEA-Cl, 2.5 MgATP, 0.25 Na_3GTP,1 QX-314 [Sigma-Aldrich], pH 7.2–7.4; 285–295 mOsm). For mEPSCs, membrane potential was held at −65 mV and perfusion was switched to ACSF containing tetrodotoxin (TTX, 1μM, Tocris, Ellisville, MO) and picrotoxin (100 μM, Sigma-Aldrich). For mIPSCs, membrane potential was held at 0 mV and perfusion was switched to ACSF containing TTX (1μM), D-APV (50 μM, Tocris), and NBQX (2 μM, Tocris). Cells were allowed to stabilize after starting toxin-containing solutions for at least 10 min. Due to possible effects of action potential blockade on synaptic properties (Turrigiano, 2008), all mEPSC and mIPSC recordings were made within 30 min after TTX was introduced to the slice. For miniature event analysis, 200 sequential events from each cell were individually identified visually using Clampfit 10.2 software (Molecular Devices, Sunnyvale, CA). Events were at least 10 pA, and the baseline amplitude was adjusted for each event to mid signal at the initiation time of the event.

In another set of animals, APs were recorded in current-clamp mode with “resting” membrane potentials normalized to −70 mV. For these recordings, pipettes were filled with potassium-based solution (in mM: 130 K-methanesulfate, 10 KCl, 10 HEPES, 0.4 EGTA, 2.0 $MgCl_2$, 2.5 MgATP, 0.25 Na_3GTP, pH 7.2–7.4; 285–295 mOsm). At least 10 minutes after initiation of the whole-cell mode, 600 ms current steps were injected from −200 pA to 225 pA in 25 pA increments with an interpulse interval of 10 s. Only cells with stable AP numbers were included in data analysis. Three runs were averaged for each cell. The

majority of recorded cells (>90%) were regular spiking (steady increase from a low number of AP with increasing current); only these cells were used for final analysis.

4.5. Statistics

For quantification of sleep time and power, 2-factor ANOVA with repeated measures was used to assess major effects of treatment. The multiple imputation method was used for missing values in power data time bins with no NREM sleep. Where ANOVA indicated a significant effect, paired Student's t-tests were used for *post hoc* analysis to assess differences between treatments at individual time points. For quantification of patch clamp recordings, cell based statistic were used; however, we also examined this data after reducing variability by averaging into animal based bins. There were no differences in outcomes of significance. The non-parametric Kolmogorav-Smirnov test was used to assess cumulative frequency distributions of post synaptic currents. The statistical software SPSS (Somer, NY) was used for analysis. Probability less than 0.05 was considered significant.

Acknowledgments

This work was supported by NIH DA023206 (YD), NS025378 (JK) and NS031453 (JK) and the Humboldt Foundation (YD).

Abbreviations

SD	Sleep deprivation
PFC	prefrontal cortex
mPFC	medial prefrontal cortex
mEPSC	miniature excitatory postsynaptic current
mIPSC	miniature inhibitory postsynaptic current
EMG	elecromyogram
EEG	electroencephalogram
REM	rapid eye movement
NREM	non-rapid eye movement
TTX	artificial cerebral spinal fluid, tetrodotoxin
AP	action potential
AMPA	α-amino-3-hydroxy-5-methyl-4-isoxazolepropionic acid
AHP	afterhyperpolarization

References

Berendse HW, Galis-de Graaf Y, Groenewegen HJ. Topographical organization and relationship with ventral striatal compartments of prefrontal corticostriatal projections in the rat. J Comp Neurol. 1992; 316:314–347. [PubMed: 1577988]

Bodosi B, Obal F Jr. Gardi J, Komlodi J, Fang J, Krueger JM. An ether stressor increases REM sleep in rats: possible role of prolactin. Am J Physiol Regul Integr Comp Physiol. 2000; 279:R1590–1598. [PubMed: 11049840]

Chuah YML. The Neural Basis of Interindividual Variability in Inhibitory Efficiency after Sleep Deprivation. Journal of Neuroscience. 2006; 26:7156–7162. [PubMed: 16822972]

Crick F, Mitchison G. The function of dream sleep. Nature. 1983; 304:111–114. [PubMed: 6866101]

Davis CJ, Meighan PC, Taishi P, Krueger JM, Harding JW, Wright JW. REM sleep deprivation attenuates actin-binding protein cortactin: A link between sleep and hippocampal plasticity. Neuroscience Letters. 2006; 400:191–196. [PubMed: 16533564]

Finelli LA, Baumann H, A.A. B, Achermann P. Dual Electroencephalogram Markers of Human Sleep Homeostasis: Correlation Between Theta Activity in Waking and Slow-Wave Activity in Sleep. Neuroscience. 2000; 101:523–529. [PubMed: 11113301]

Goldman-Rakic PS. Cellular Basis of Working Memory. Neuron. 1995; 14:477–485. [PubMed: 7695894]

Graves LA. Sleep Deprivation Selectively Impairs Memory Consolidation for Contextual Fear Conditioning. Learning & Memory. 2003; 10:168–176. [PubMed: 12773581]

Groenewegen HJ, Berendse HW, Wolters JG, Lohman AH. The anatomical relationship of the prefrontal cortex with the striatopallidal system, the thalamus and the amygdala: evidence for a parallel organization. Prog Brain Res. 1990; 85:95–116. discussion 116-118. [PubMed: 2094917]

Groenewegen HJ, Uylings HB. The prefrontal cortex and the integration of sensory, limbic and autonomic information. Prog Brain Res. 2000; 126:3–28. [PubMed: 11105636]

Grossberg, S. Towards a Unified Theory of Neocortex: Laminar Cortical Circuits for Vision and Cognition. Cisek, P.; Drew, T.; Kalaska, J., editors. Elsevier; Amsterdam: 2006.

Hille, B. Ion Channels of Excitable Membranes. Sinauer Associates; 2001.

Huang YH, Lin Y, Mu P, Lee BR, Brown TE, Wayman G, Marie H, Liu W, Yan Z, Sorg BA. In Vivo Cocaine Experience Generates Silent Synapses. Neuron. 2009; 63:40–47. [PubMed: 19607791]

Ishikawa M, Mu P, Moyer JT, Wolf JA, Quock RM, Davies NM, Hu X. t. Schluter OM, Dong Y. Homeostatic Synapse-Driven Membrane Plasticity in Nucleus Accumbens Neurons. Journal of Neuroscience. 2009; 29:5820–5831. [PubMed: 19420249]

Kapas L, Bohnet SG, TTraynor TR, Majde JA, Szentirmai E, Magrath P, Taishi P, Krueger JM. Spontaneous and influenza virus-induced sleep are altered in TNF-double-receptor deficient mice. Journal of Applied Physiology. 2008; 105:1187–1198. [PubMed: 18687977]

Killgore WD. Effects of sleep deprivation on cognition. Prog Brain Res. 2010; 185:105–129. [PubMed: 21075236]

Krueger JM, Kapas L, Kimura M, Opp MR. Somnogenic Cytokines: Methods and Overview. Methods in Neurosciences. 1993; 17:111–129.

Krueger JM, Obal F. A neuronal group theory of sleep function. J Sleep Res. 1993; 2:63–69. [PubMed: 10607073]

Krueger JM, Rector DM, Roy S, Van Dongen HPA, Belenky G, Panksepp J. Sleep as a fundamental property of neuronal assemblies. Nature Reviews Neuroscience. 2008; 9:910–919.

Lante F, Toledo-Salas JC, Ondrejcak T, Rowan MJ, Ulrich D. Removal of Synaptic Ca2+-Permeable AMPA Receptors during Sleep. Journal of Neuroscience. 2011; 31:3953–3961. [PubMed: 21411638]

Le Marec N, Beaulieu I, Godbout R. Four hours of paradoxical sleep deprivation impairs alternation performance in a water maze in the rat. Brain Cogn. 2001; 46:195–197. [PubMed: 11527327]

Liu ZW, Faraguna U, Cirelli C, Tononi G, Gao XB. Direct Evidence for Wake-Related Increases and Sleep-Related Decreases in Synaptic Strength in Rodent Cortex. Journal of Neuroscience. 2010; 30:8671–8675. [PubMed: 20573912]

Marshall L, Born J. The contribution of sleep to hippocampus-dependent memory consolidation. Trends in Cognitive Sciences. 2007; 11:442–450. [PubMed: 17905642]

Massimini M. The Sleep Slow Oscillation as a Traveling Wave. Journal of Neuroscience. 2004; 24:6862–6870. [PubMed: 15295020]

Mauzur A, Pace-Schott EF, Hobson AJ. The Prefrontal Cortex in Sleep. Trends in Cognitive Sciences. 2002; 11:475–481.

McDermott CM. Sleep deprivation-induced alterations in excitatory synaptic transmission in the CA1 region of the rat hippocampus. The Journal of Physiology. 2005; 570:553–565. [PubMed: 16322058]

McDermott CM, LaHoste GJ, Chen C, Musto A, Bazan NG, Magee JC. Sleep Deprivation Causes Behavioral, Synaptic, and Membrane Excitability Alterations in Hippocampal Neurons. The Journal of Neuroscience. 2003; 23:9687–9695. [PubMed: 14573548]

Miller E, Cohen JD. An Integrative Theory of Prefrontal Cortex Function. Annual Review of Neuroscience. 2001; 24:167–202.

Nieuwenhuis ILC, Takashima A. The role of the ventromedial prefrontal cortex in memory consolidation. Behavioural Brain Research. 2011; 218:325–334. [PubMed: 21147169]

Palchykova S, Winskysommerer R, Meerlo P, Durr R, Tobler I. Sleep deprivation impairs object recognition in mice. Neurobiology of Learning and Memory. 2006; 85:263–271. [PubMed: 16423541]

Paxinos, G.; Franklin, KBJ. The Mouse Brain in Stereotaxic Coordinates. Academic Press; San Diego: 2001.

Robbins TW. Chemistry of the mind: Neurochemical modulation of prefrontal cortical function. The Journal of Comparative Neurology. 2005; 493:140–146. [PubMed: 16254988]

Sesack SR, Deutch AY, Roth RH, Bunney BS. Topographical organization of the efferent projections of the medial prefrontal cortex in the rat: an anterograde tract-tracing study with Phaseolus vulgaris leucoagglutinin. J Comp Neurol. 1989; 290:213–242. [PubMed: 2592611]

Smith C, Rose GM. Evidence for a paradoxical sleep window for place learning in the Morris water maze. Physiol Behav. 1996; 59:93–97. [PubMed: 8848497]

Steriade M. Grouping of brain rhythms in corticothalamic systems. Neuroscience. 2006; 137:1087–1106. [PubMed: 16343791]

Szentirmai E, Kapas L, Sun Y, Smith RG, Krueger JM. The preproghrelin gene is required for the normal integration of thermoregulation and sleep in mice. Proceedings of the National Academy of Sciences. 2009; 106:14069–14074.

Tartar JL, McKenna JT, Ward CP, McCarley RW, Strecker RE, Brown RE. Sleep fragmentation reduces hippocampal CA1 pyramidal cell excitability and response to adenosine. Neuroscience Letters. 2010; 469:1–5. [PubMed: 19914331]

Thomas M, Sing H, Belenky G, Holcomb H, Mayberg H, Dannals R, Wagner H, Thorne D, Popp K, Rowland L, Welsh A, Balwinski S, Redmond D. Neural Basis of Cognitive Performance Impairments During Sleepiness. I. Effects of 24 h of Sleep Deprivation on Waking Human Reginal Brain Activity. Journal of Sleep Research. 2000; 9:335–352. [PubMed: 11123521]

Tononi G, Cirelli C. Sleep function and synaptic homeostasis. Sleep Medicine Reviews. 2006; 10:49–62. [PubMed: 16376591]

Turrigiano GG. The Self-Tuning Neuron: Synaptic Scaling of Excitatory Synapses. Cell. 2008; 135:422–435. [PubMed: 18984155]

Turrigiano GG, Leslie KR, Desai NS, Rutherford LC, Nelson SB. Activity-dependent scaling of quantal amplitude in neocortical neurons. Nature. 1998; 391:892–896. [PubMed: 9495341]

Vyazovskiy VV, Olcese U, Lazimy YM, Faraguna U, Esser SK, Williams JC, Cirelli C, Tononi G. Cortical Firing and Sleep Homeostasis. Neuron. 2009; 63:865–878. [PubMed: 19778514]

Wu JC, Gillin JC, Buchsbaum MS, Chen P, Keator DB, Wu N. Khosla, Darnall LA, Fallon JH, Bunney WE. Frontal Lobe Metabolic Decreases with Sleep Deprivation not Totally Reversed by Recovery Sleep. Neuropsychopharmacology. 2006; 31:2783–2792. [PubMed: 16880772]

Yan J, Li J-C, Xie M-L, Zhang D, Qi A-P, Hu B, Huang W, Xia J-X, Hu Z-A. Short-term sleep deprivation increases intrinsic excitability of prefrontal cortical neurons. Brain Research. 2011; 1401:52–58. [PubMed: 21663896]

Yang R-H, Wang W-T, Hou X-H, Hu S-J, Chen J-Y. Ionic mechanisms of the effects of sleep deprivation on excitability in hippocampal pyramidal neurons. Brain Research. 2010; 1343:135–142. [PubMed: 20471377]

Highlights

- Sleep loss induces adaptations in deep layer pyramidal cells of the mouse prefrontal cortex
- miniature excitatory post synaptic current amplitude slightly reduced
- miniature inhibitory post synaptic currents unaffected
- Intrinsic membrane excitability increased

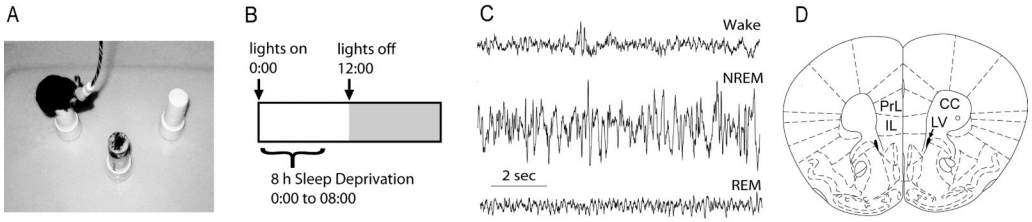

Figure 1.

Sleep deprivation and methodology. **A**, Photo showing an EEG-equipped mouse in the SD chamber. **B**, Diagram illustrating the light dark cycle and SD period. **C**, EEG traces showing typical wake (top), NREM sleep (middle), and REM sleep patterns. **D**, Mouse brain atlas plate (Paxinos and Franklin, 2001) showing the location of the infralimbic (IL) and prelimbic (PrL) regions of the PFC relative to the corpus callosum (CC) and lateral ventricle (LV).

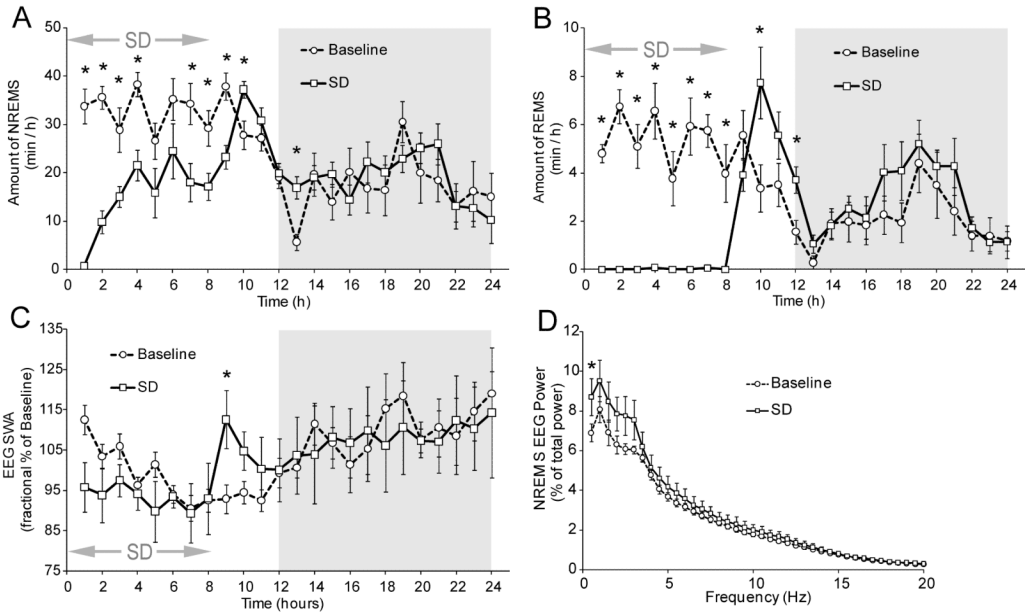

Figure 2.

A, NREM sleep for 24 h including the SD period (arrows) in 1 h bins. Shaded area is the dark period. **B**, REM sleep for 24 h including the SD period in 1 h bins. **C**, NREM sleep delta power for 24 h including the SD period in 1 h bins. **D**, NREM sleep power spectra for the first h after SD (time bin 9). Error bars ±SEM. * denotes $p<0.05$

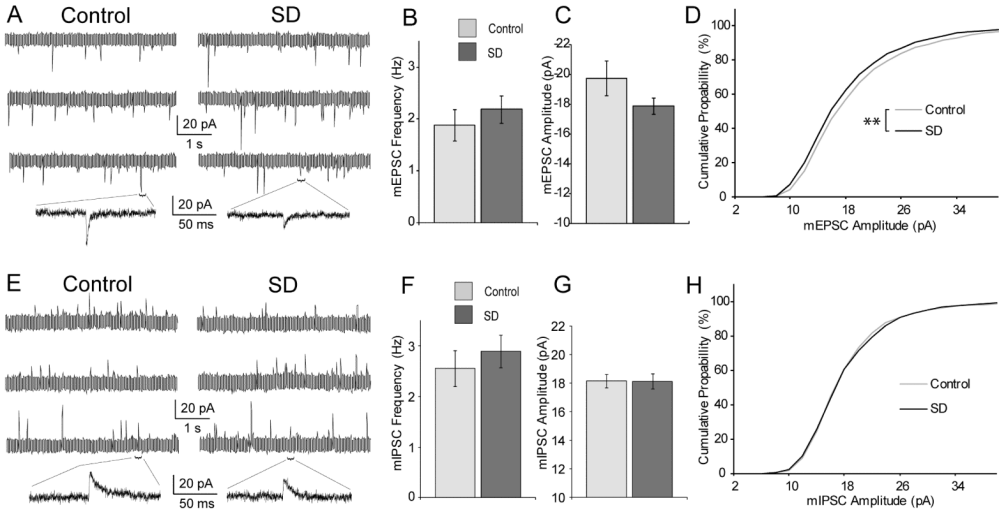

Figure 3.

Synaptic effects of SD. **A**, Example traces for mEPSCs with and without SD (3 cells each) and enlarged regions below to show single events. Note that noise levels appear larger in highly compressed sweeps. **B**, Average mEPSC frequency. **C**, Average mEPSC amplitude. **D**, Cumulative probability distribution of mEPSCs. **E**, Example traces for mIPSCs with and without SD. **F**, Average mIPSC frequency. **G**, Average mIPSC amplitude. **H**, Cumulative probability distribution of mIPSCs. Error bars ±SEM. ** denotes $p<0.01$

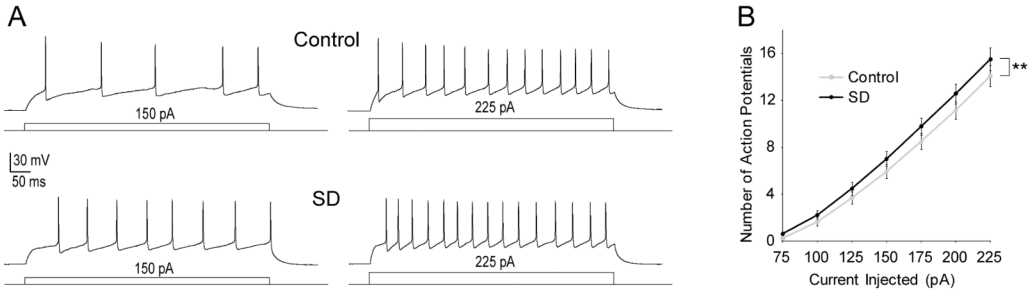

Figure 4.

Intrinsic membrane effects of SD. **A**, Action potential firing example traces at 150 and 225 pA injected current for control (top) and SD. **B**, Average number of action potentials for control and SD. Error bars ±SEM, ** denotes $p<0.01$.

Table 1

Intrinsic property averages ±SEM for control and SD group cells.

Parameter	Control (n=22)	SD (n=27)
Break-in RMP (mV)	−69.71 ±1.76	−69.26 ±1.05
Stabilized RMP (mV)	−54.73 ±1.97	−55.41 ±1.54
R_i at −100 pA (MΩ)	223.79 ±7.41	238.40 ±8.89
R_i at +25 pA (MΩ)	329.77 ±16.33	323.76 ±16.59
Latency 1st spike (ms)	406.89 ±25.30	433.36 ±19.39
Rheobase (pA)	101.14 ±5.06	99.07 ±5.08
AP Threshold (mV)	−33.50 ±0.93	−35.14 ±0.61
AP Amplitude (mV)	70.70 ±1.27	69.75 ±1.56
AP Halfwidth (ms)	0.98 ±0.03	0.98 ±0.03